ACS Catalysis

pubs.acs.org/acscatalysis Research Article

Concerted Cycloaddition Mechanism in the CuAAC Reaction Catalyzed by 1,8-Naphthyridine Dicopper Complexes

Julie Héron and David Balcells*

Cite This: *ACS Catal.* 2022, 12, 4744–4753 Read Online

ACCESS | Metrics & More | Article Recommendations | Supporting Information

ABSTRACT: Copper-catalyzed azide-alkyne cycloaddition (CuAAC) is one of the most versatile reactions in the "click chemistry" toolbox, and its development has made the synthesis of 1,4-triazole derivatives robust and efficient. In this work, we present a density functional theory (DFT) study on the mechanism of the CuAAC reaction catalyzed by a dicopper complex supported by a nonsymmetric 1,8-naphtyridine ligand bearing two different metal-coordinating substituents (i.e., $-P(tBu)_2$ and $-C(Me)(Py)_2$). The calculations showed that the cycloaddition of the azide to the alkyne occurs in a single concerted step, in contrast with the two-step mechanism proposed in the literature. The energies predicted for this step indicated that the 1,4-triazole isomer of the product is formed in a selective manner, in agreement with experiments. Further, the DFT results showed that there is a subtle and complex interplay between several variables, including the relative orientation of the two substrates, the position of the counter-anion, and the partial decoordination of the 1,8-naphtyridine ligand. A series of 90 transition state calculations showed that, on average, the impact of these variables is strong on the structures but soft on the energy barriers, highlighting the flexible nature of the bonding within the coordination sphere of the bimetallic core of the catalyst. The insight provided by this study will be valuable for the further development of dicopper catalysts for the CuAAC reaction.

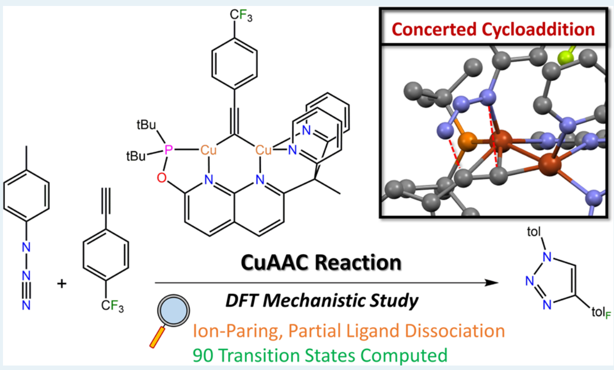

KEYWORDS: *CuAAC, cycloaddition, mechanism, DFT, C−H activation, ion-pairing, ligand dissociation*

INTRODUCTION

The copper-catalyzed cycloaddition of azides with terminal alkynes (CuAAC) yields 1,4-di-substituted 1,2,3-triazoles. It was first reported by Tornøe et al.[1] and Rostovtsev et al.[2] in 2002 and has had a wide variety of applications[3,4] in chemistry,[5−12] materials science,[13−20] and biology[21−27] during the last 20 years. This reaction is one of the most relevant examples of click chemistry,[28] a branch of organic synthesis focused on the development of reactions linking building blocks via cross-couplings, cycloadditions, and other reactions forming carbon-heteroatom bonds.

The CuAAC reaction[29−34] is atom-efficient and produces selectively 1,4-triazoles with high yields (often >95%) at room temperature, and side products[2,35−38] are rarely observed. It is also very robust because it can support a wide pH range (4−12) and various solvents (organic and water), and almost any type of functional group is tolerated on both the azide and alkyne. The catalyst for this reaction is usually a small amount of an inexpensive Cu^{II} salt (e.g., $CuSO_4$) in the presence of sodium ascorbate to produce the Cu^{I} active species. All these characteristics make the CuAAC reaction a very efficient, cheap, and robust synthetic approach to 1,4 triazoles.

The mechanism of the CuAAC reaction was initially assumed to be monomeric;[2,39−41] the active species in the catalytic cycle involve only one copper center. However, the number of coppers engaged in the reaction started to be a question in 2005, with the publication of a kinetic study[42] showing second order in copper. Because copper salts are often used in the presence of ligands generating the catalyst in situ, a large variety of complexes are potentially accessible in solution, ranging from mononuclear complexes to clusters with polynuclear cores. Several experimental and computational studies[43−57] suggested that dicopper species are more active than their monomeric counterparts, thus being the actual active species. The mechanism of the CuAAC reaction starts with the reduction[58] of the Cu^{II} salts to Cu^{I} active species entering the catalytic cycle. The reduction can occur via the addition of a reducing agent (like sodium ascorbate) or via the

Received: February 10, 2022
Revised: March 28, 2022
Published: April 6, 2022

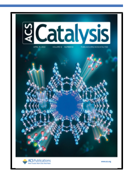

https://doi.org/10.1021/acscatal.2c00723
ACS Catal. 2022, 12, 4744–4753

Glaser Hay homocoupling of alkynes. The actual catalytic cycle (Figure 1) starts with a Cu^I-alkynyl complex coordinating to the second Cu^I complex. An important feature of this mechanism is that the cycloaddition of the azide to the resulting dicopper species is a stepwise process[44,49] involving the following reactions: (1) azide coordination to the dicopper core yielding the first C−N bond in a six-membered metallacycle, followed by (2) intramolecular C−N bond formation yielding the triazolyl-Cu^I intermediate and dissociating one of the two coppers. In the final step, a proton transfer from the alkyne to the triazolyl ligand allows for the regeneration of the alkynyl Cu^I complex and the release of the 1,4-triazole product.

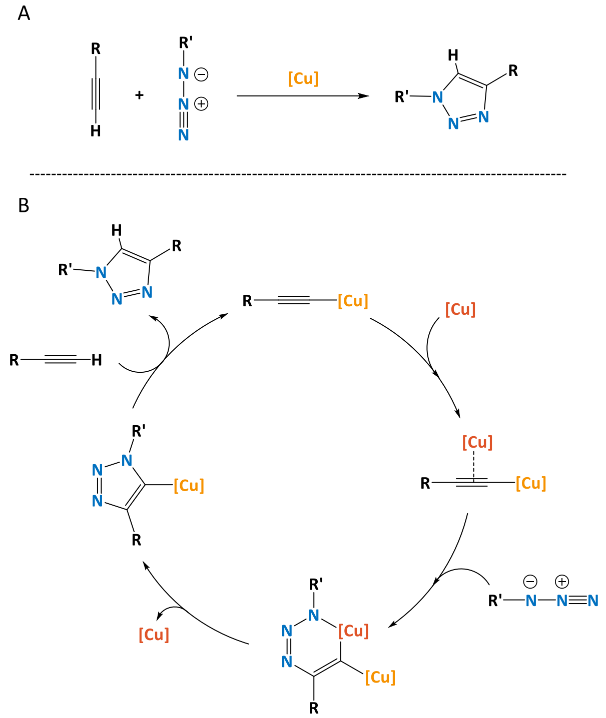

Figure 1. CuAAC reaction (A) and its mechanism with dinuclear active species (B).

Because of the flexibility of the system, the exact geometries of the active species can vary depending on the ligands and the reaction conditions, but the general steps remain the same.[43−46,49,50,59−61] The rate-determining step (RDS) depends also on the reaction conditions.[60] In aprotic conditions, the proton transfer from the alkyne to the triazolyl complex happens in one concerted step and is the RDS. However, under protic conditions, the deprotonation of the alkyne and the protonation of the triazolyl are decoupled in two different steps, and their respective transition states are stabilized compared to the concerted one. Thus, in the whole cycle, there are three transition states[60] (deprotonation, cyclization, protonation) with similar energies, and therefore, the RDS can vary easily depending on specific reaction conditions and on the environment around the coppers. The origin of the selectivity of this reaction was already discussed in great length in the case of the copper catalyst salts.[41,62] The transition state of the 1,5 cyclization is higher in energy than the 1,4 one because of the higher distortion needed to align the atoms and the alignment of the charges of the carbons and nitrogens that are less ideal than those for the 1,4 cyclization.

There is a large variety of ligands used for the CuAAC reaction, and they serve a double purpose: to stabilize the Cu^I center to avoid deactivation (preventing disproportionation into Cu^0 and Cu^{II}) and to make the reaction more efficient. The most commonly used ligands are acetate,[53,58,63,64] NHC,[40,51,54,55,65−67] polydentate amines/heterocycles,[68−72] and phosphines.[56,57,73] Some ligands can coordinate two coppers (like the ones based on acetate or 1,8 naphthyridine[74,75]), promoting the formation of bimetallic active species.

Overall, the mechanism of the CuAAC reaction is well known for Cu^{II} catalyst salts, and the nature and the order of the elementary step composing the catalytic cycle remain unchanged regardless of the system. However, the reaction is also extremely flexible because the nature of the active species can vary (nuclearity, composition, and geometry), adapting to the substrates and reaction conditions. The efficiency and robustness of this reaction lie in its adaptable behavior.

A previous study[76] from our group described the properties of a dicopper complex based on a 1,8-naphthyridine ligand ($[Cu_2(DPEOPN)(\mu\text{-}Ph)]^+.NTf_2^-$, $\mathbf{1^+.NTf_2^-}$ in Figure 2;

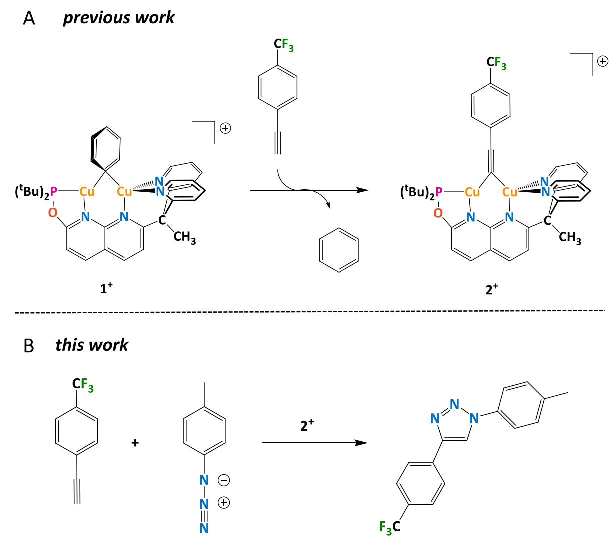

Figure 2. C−H activation of alkynes by $\mathbf{1^+}$ (A) and CuAAC reaction catalyzed by $\mathbf{2^+}$ (B).

NTf_2^- = bistriflimide). This complex activates the C−H bond of alkynes via a concerted proton transfer between the alkyne and the bridging phenyl, leading to the release of benzene and the alkynyl-bridged dicopper complex $\mathbf{2^+.NTf_2^-}$ ($[Cu_2(DPEOPN)(\mu\text{-}CC(\rho\text{-}CF_3\text{-}C_6H_4)]^+.NTf_2^-$).

A similar proton transfer producing copper alkynyl complexes happens in the CuAAC reaction mechanism (Figure 1). In this article, we report a computational study on the CuAAC reaction catalyzed by $\mathbf{2^+}$. The catalytic properties of $\mathbf{2^+}$ have not been reported experimentally, but a complex with a symmetric naphthyridine ligand is known to catalyze this reaction with similar substrates (90% yield in the cycloaddition of *p*-tolylazide to *p*-tolylacetylene at 100 °C during 5.3 h in *o*-1,2-difluorobenzene).[74] The main motivation for studying $\mathbf{2^+}$ is the nonsymmetric nature of its naphthyridine ligand, which, in contrast with symmetric ligands, differentiates the two metal centers. The calculations revealed a mechanism that is significantly different from those proposed for Cu^{II} salts, including a concerted cycloaddition step. The impact of the

https://doi.org/10.1021/acscatal.2c00723
ACS Catal. 2022, 12, 4744−4753

environment of copper on the reaction is also described, including partial ligand decoordination and counterion effects, as well as the origin of the selectivity and the pathways leading to catalyst poisoning.

■ COMPUTATIONAL DETAILS

DFT calculations were carried out with the hybrid PBE0 GGA functional,[77] as implemented in the Gaussian16 software package.[78] The Grimme dispersion model GD3[79] was used. Two different basis sets,[80,81] one of double-ζ quality (def2SVP) and one of triple-ζ quality (def2TZVP), were used. All the structures were fully optimized without any geometry or symmetry constraint with the def2SVP basis set. Frequency calculations were also carried out with the same basis set, to confirm the energy-minimum nature of all stationary points (i.e., all-real frequencies) and to estimate the thermal corrections at 298.15 K (E_T, including zero-point, thermal, and entropy energies). A selection of transition states was relaxed with IRC (Intrinsic Reaction Coordinate) calculations to verify that they belong to the reaction pathway. The potential energy of the optimized geometries was refined by means of single-point calculations with the def2TZVP basis set (E). The ultrafine (99,590) pruned grid was used in all calculations for higher accuracy in the computation of the two-electron integrals. All calculations, including both geometry optimization and energy refinement, were performed in THF (tetrahydrofuran) with the CPCM (conductor-like polarizable continuum model) model,[82,83] unless otherwise specified in the text. The free energies reported in the manuscript (G) were obtained by adding the thermal corrections to the refined potential energies, as shown in eq 1, and corrected to the 1 M standard state.

$$G = E + E_T \qquad (1)$$

This computational methodology was benchmarked in a previous study.[76]

■ RESULTS AND DISCUSSION

The CuAAC reaction is well known in the case of Cu^{II} catalyst salts, including the characterization of the key intermediates, both experimentally and computationally (Figure 1).[40,43,44,46,49−51,54,60,84] Based on this knowledge, four intermediates were considered for building a tentative catalytic cycle for our system (Figure 3). The first intermediate is **2**$^+$, in which the alkynyl is already bound to the two coppers in a bridging position. The second intermediate (**3**$^+$) results from the coordination of the azide to **2**$^+$. The third intermediate (**4**$^+$) is a six-membered ring metallacycle resulting from the formation of the first C−N bond. The fourth and last intermediate (**5**$^+$) originates from the formation of the second C−N bond and corresponds to a triazolyl bridging the two coppers. A proton transfer between this last intermediate and the alkyne regenerates **2**$^+$, releasing the 1,4 triazole product. To ease the description of these complexes, we used the atom labels shown in Figure 4.

In the geometry optimization of the four intermediates postulated in Figure 3, only three converged as energy minima, that is, **2**$^+$, **3**$^+$, and **5**$^+$ (Figures S2, S4, and S5). The metallacycle intermediate **4**$^+$ could not be optimized despite numerous attempts, which, in all instances, converged into **5**$^+$. The lack of convergence in the optimization of **4**$^+$ can be ascribed to the steric clash between the substrate substituents and the phosphine and pyridine arms of the DPEOPN ligand.

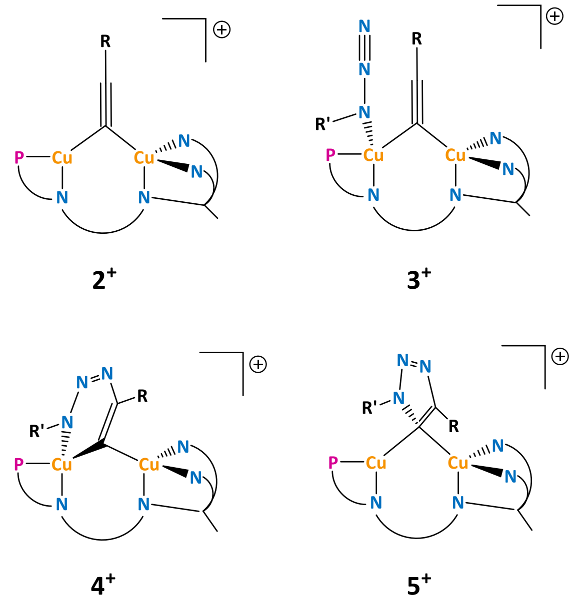

Figure 3. Four intermediates considered for the mechanism of the CuAAC reaction catalyzed by **2**$^+$.

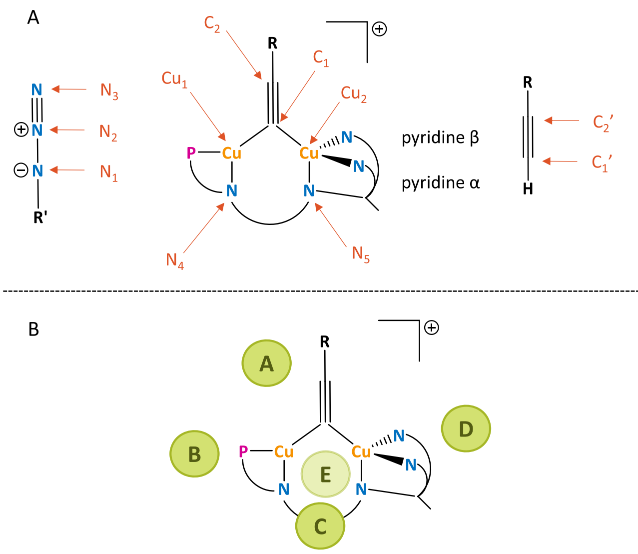

Figure 4. Atom labels (A) and positions **A**−**E** of NTf_2^- around 2^+. Positions **C** and **E** become inequivalent after the coordination of the azide substrate. All five positions introduce a −1 charge, making the overall system neutral.

Thus, the cyclization step for the CuAAC reaction catalyzed by **2**$^+$ follows a mechanism different from that proposed for Cu^{II} salts.

In **2**$^+$, DPEOPN is fully coordinated to the coppers and the alkynyl bridges the metals symmetrically with a $Cu−C_1$ distance of 1.95 Å. The coppers are separated to a distance of 2.39 Å. To obtain **3**$^+$, the azide coordinates to the copper on the phosphine side with a $Cu_1−N_1$ distance of 2.29 Å. It cannot coordinate to the other copper because of the steric hindrance with the pyridine (Figure S3). The coordination of the azide breaks the symmetry of the $Cu_1−C_1−Cu_2$ bridge (2.04 and 1.92 Å). **5**$^+$ has a geometry similar to **2**$^+$, with the triazolyl moiety bridging the coppers (2.02 Å).

Two different structural factors, that is, the partial dissociation of DPEOPN and the pairing with the counterion

https://doi.org/10.1021/acscatal.2c00723
ACS Catal. 2022, 12, 4744−4753

(NTf_2^-), were systematically explored for 2^+, 3^+, and 5^+. DPEOPN is a labile ligand undergoing partial dissociation by decoordination of one of the pyridines.[76] The resulting complexes (and associated transition states) were labeled $\mathbf{X}_\alpha^+$ or $\mathbf{X}_\beta^+$ ($\mathbf{TS}_{X\alpha}$ or $\mathbf{TS}_{X\beta}$; X = **2**, **3**, or **5**), depending on which of the two pyridines, $\boldsymbol{\alpha}$ or $\boldsymbol{\beta}$, is dissociated (Figure 4). These dissociations are slightly endoergic, with an energy cost ranging from +1.5 to +2.9 kcal/mol (Tables S1 and S2). The impact of the pyridine dissociations onto the structure of these complexes is rather small in most cases. The largest distortions are observed in the Cu_1-Cu_2 distance, with a maximum variation of +0.2 Å in $\mathbf{3}_\alpha^+$, and in the distance between the coppers and DPEOPN, with a maximum variation of +0.12 Å, also in $\mathbf{3}_\alpha^+$.

The interaction of the counterion with the complexes was examined by computing the free energy of the association reaction yielding the ion pair. Multiple positions (Y = **A**−**E**) of NTf_2^- around the complexes were considered (Figure 4), and the corresponding complexes (and transition states) were labeled $\mathbf{X}_\mathbf{Y}$ and $\mathbf{TS}_{\mathbf{ZY}}$ (X = **2**, **3**, or **5** for the intermediates and Z = **1** to **6** for the transition state series). The Y spatial positions of the counterion around the catalyst were formulated after considering the three-dimensional shape of the system; that is, above the alkynyl bridge (**A**), at the P and N_2 chelating sides of the ligand (**B** and **D**), and above and below the naphthyridine plane (**C** and **E**). After placing the counterion in these positions, the geometries were fully relaxed to either energy minima (intermediates) or saddle points (transition states). The association energies range from −4.5 to +3.0 kcal/mol, with $\mathbf{2_B}$, $\mathbf{3_E}$, and $\mathbf{5_E}$ being the most stable. All three intermediates undergo an exergonic association with NTf_2^- for at least one of the five possible **A**−**E** positions. Ion pairing did not alter the geometries of the corresponding cationic complexes to any great extent because NTf_2^- does not coordinate to the coppers, interacting with the complexes only via weak interactions. In $\mathbf{2_B}$, NTf_2^- is close to the ^{t}Bu substituents of the phosphine (Figure 5). In $\mathbf{3_E}$ and $\mathbf{5_E}$, the counterion is located in the cavity formed by the two arms of DPEOPN, maximizing its interaction with the ligand. NTf_2^- also interacts with the tolyl substituent of the azide in $\mathbf{3_E}$ and of the triazolyl in $\mathbf{5_E}$. For these three complexes, the combination of the partial dissociation of DPEOPN with the association with NTf_2^- did not yield energies lower than the ones obtained considering only ion-pairing (Tables S1 and S2).

The most stable complexes $\mathbf{2_B}$, $\mathbf{3_E}$, and $\mathbf{5_E}$ were arranged in the tentative catalytic cycle shown in Figure 6. This mechanism involves three steps: (A) the coordination of the azide to $\mathbf{2_B}$, yielding $\mathbf{3_E}$, (B) the cyclization between the alkynyl and the azide in $\mathbf{3_E}$, yielding $\mathbf{5_E}$, and (C) the proton transfer from the alkyne to $\mathbf{5_E}$, yielding the triazole product and closing the cycle. Thermodynamics computed for this catalytic cycle showed that the coordination of the azide is thermoneutral, with $\mathbf{3_E}$ lying at −0.8 kcal/mol below $\mathbf{2_B}$, whereas the cyclization step is very exergonic, with $\mathbf{5_E}$ lying at −53.9 kcal/mol below $\mathbf{2_B}$.

A relaxed scan on the coordination of the azide to $\mathbf{2_B}$ (step A in Figure 6) did not show any energy maximum, thus suggesting that this reaction has no significant barrier in the potential energy surface (Figure S8). In contrast, for step B, the calculations converged into a cycloaddition transition state involving the formation of the two C−N bonds in a concerted fashion ($\mathbf{TS_1}$). The impact of the partial dissociation of DPEOPN and the association with the counterion was investigated for this step, resulting in a series of 18 transition

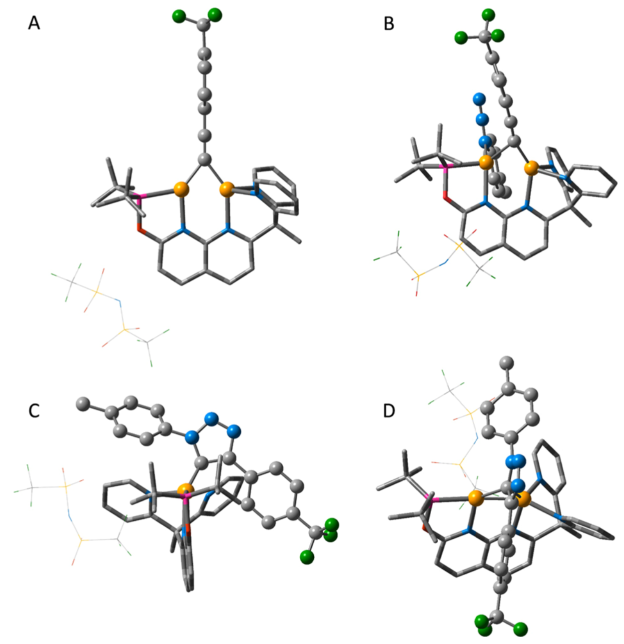

Figure 5. DFT-optimized geometries of the intermediates $\mathbf{2_B}$ (A), $\mathbf{3_E}$ (B), and the side (C), and front (D) views of $\mathbf{5_E}$. All H atoms were removed for clarity. Representation: ball-and-stick (Cu, alkynyl, azide, and triazolyl), tube (DPEOPN), and wire (NTf_2^-). Selected distances, in Å, for $\mathbf{2_B}$, $\mathbf{3_E}$, and $\mathbf{5_E}$, respectively: Cu···Cu (2.38, 2.46, 2.41), Cu−C_μ ($1.97_P/1.95_{N2}$, $2.05_P/1.92_{N2}$, $2.02_P/2.03_{N2}$), Cu−P (2.25, 2.27, 2.26), and Cu−N_{Py} (2.08/2.08, 2.11/2.11, 2.08/2.09).

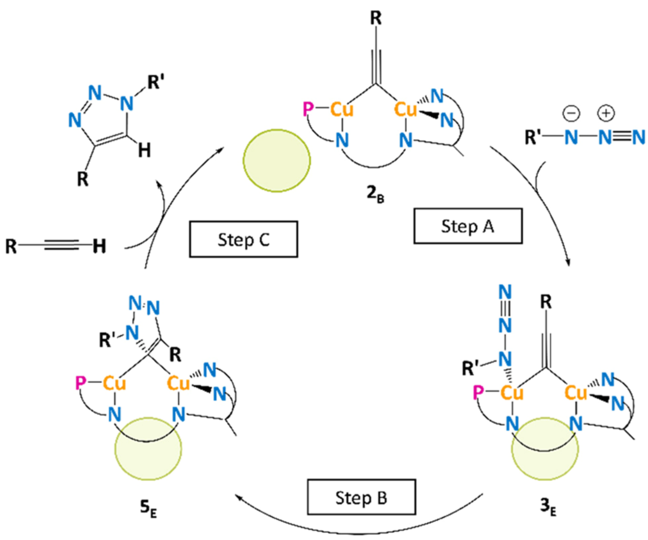

Figure 6. Tentative catalytic cycle for the CuAAC reaction using 2^+ as the catalyst. Green spheres illustrate the position of NTf_2^- in each calculated structure.

states (Figures S10 and S11). Overall, these transition states are within a wide range of energies: 20.0−27.3 kcal/mol. The transition state with the lowest energy is $\mathbf{TS_{1E}}$, with NTf_2^- in position **E**, highlighting the importance of considering the counterion and its possible positions in the model. In addition to DPEOPN, NTf_2^- interacts with the tolyl substituent of the azide, which is located next to it (Figure 7A). The impact of the interaction with the counterion on the geometry of the transition states is minimal because most substantial distortions are within a range of ±0.05 Å for the distances.

https://doi.org/10.1021/acscatal.2c00723
ACS Catal. 2022, 12, 4744−4753

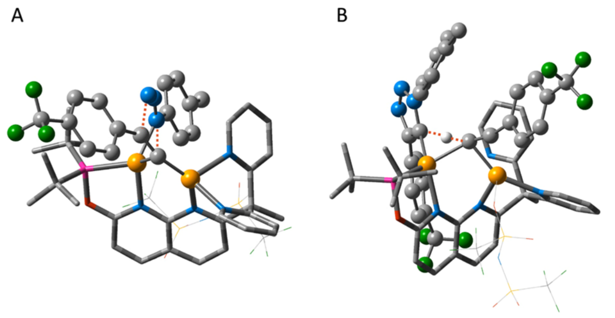

Figure 7. DFT-optimized geometries of the transition states $\mathbf{TS_{1E}}$ (A) and $\mathbf{TS_{3\beta C}}$ (B). All H atoms were removed for clarity, except the one involved in the C−H activation. Representation: ball-and-stick (Cu, alkynyl, azide, and triazolyl), tube (DPEOPN), and wire (NTf_2^-). Breaking and forming bonds are shown with a dotted red line and have these interatomic distances, in Å: In $\mathbf{TS_{1E}}$, 2.85 (N−C_μ) and 1.95 (N−C); and in $\mathbf{TS_{3\beta C}}$, 1.36 (C_μ−H) and 1.54 (H−C).

Ion pairing is slightly favorable in one case ($\mathbf{TS_{1E}}$) and isoenergetic or unfavorable in the others. The energy differences between the transition states arise from the various weak interactions with the counterion. The partial dissociation of DPEOPN yielded higher energies in all cases. The nature of the transition states was confirmed by IRC-driven relaxation on their selection, which did not yield any unexpected intermediates. The relaxation of $\mathbf{TS_{1E}}$ (Figure 7) toward products yielded the 1,4-triazolyl ring bridging the two copper centers of $\mathbf{5_E}$ (Figure 6). The concerted nature of the cycloaddition step can be ascribed to the high saturation of the two metal centers in $\mathbf{2^+}$ (Figure 5). Despite the flexible character of the copper-ligand interactions, the Cu−C, Cu−N, and Cu−P distances show that these bonds are preserved along the reaction pathway. Their presence may thus hamper the formation of additional bonds in stepwise pathways. In line with this, these pathways had been proposed for dinuclear complexes in which the metal centers were less saturated.[44,49]

The formation of the alternative isomer leading to the 1,5-triazolyl intermediate was also computed to rationalize the origin of the selectivity. The effects of ion-pairing with NTf_2^- and the partial dissociation of DPEOPN were ignored in the study of the cycloaddition selectivity for simplifying the analysis. The 1,4- and 1,5-cycloaddition energy profiles are shown in Figure 8. Both pathways start with the addition of the azide to $\mathbf{2^+}$, which yields $\mathbf{3^+}$ in the 1,4-pathway and an adduct in the 1,5, in which the azide does not coordinate to the copper but where its tolyl substituent undergoes a π-stacking interaction with the substituent of the alkynyl group. However, the azide does coordinate to the copper on the phosphine side ($d(Cu_1{-}N_3)$ = 2.26 Å) in the 1,5 transition state $\mathbf{TS_2}$ (Figure 9A). The forming bond with C_1 is much shorter in $\mathbf{TS_2}$ than in $\mathbf{TS_1}$ (2.09 versus 2.87 Å) while the forming bond with C_2 is more elongated (2.19 versus 1.94 Å). These changes cause $\mathbf{TS_2}$ to be 6.9 kcal/mol higher than $\mathbf{TS_1}$. The 1,5-triazolyl complex ($\mathbf{6^+}$, Figure 9B) is coordinated to the coppers at a similar distance from the copper (2.02 Å), but its $ArCF_3$ substituent can exhibit a CH−π interaction with one of the pyridine rings (average distance of 2.80 Å). The complex $\mathbf{6^+}$ is 9.4 kcal/mol higher than $\mathbf{5^+}$ (1,4-triazolyl complex). The higher energies for the 1,5-cycloaddition arise from the stronger steric hindrance between the azide and the alkynyl, as well as a much stronger polarization. For example, the natural charge of Cu_1 is +0.29 in $\mathbf{TS_1}$ versus +0.79 in $\mathbf{TS_2}$ (Table S3). Overall, the 1,5 cycloaddition is thermodynamically and kinetically unfavorable compared to the 1,4 one, and this reaction should produce selectively 1,4 triazole, in agreement with the experiments.[74]

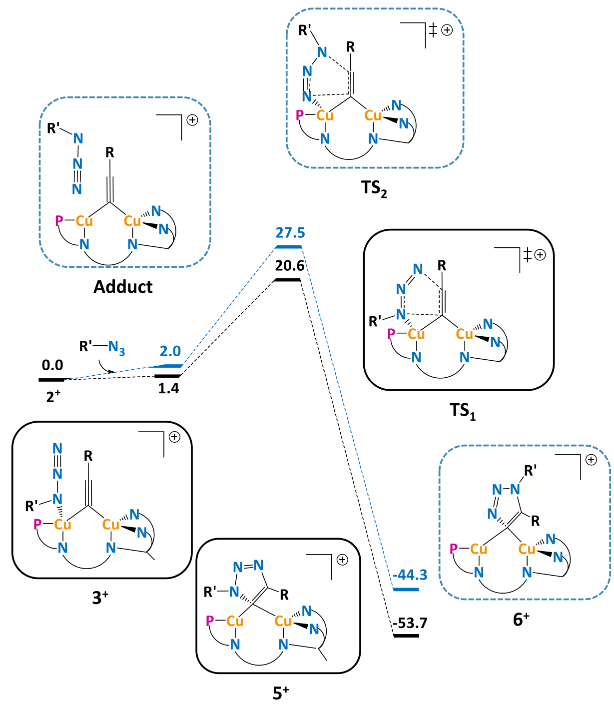

Figure 8. Energy profile for the 1,4- (solid black squares) and 1,5- (dashed blue squares) cycloaddition of the azide to $\mathbf{2^+}$. The energetics of the following C−H activation step are provided in Figure 13.

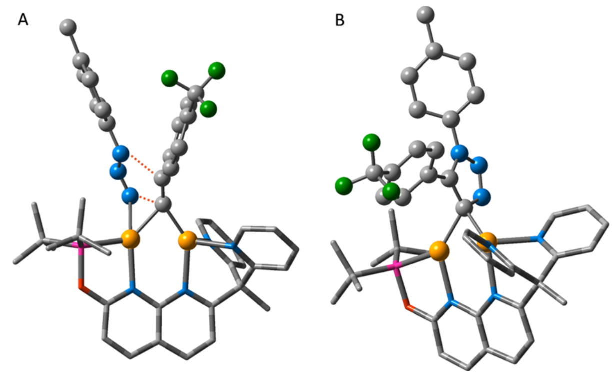

Figure 9. DFT-optimized geometries of the transition state $\mathbf{TS_2}$ (A) and of the intermediate $\mathbf{6^+}$ (B). All H atoms were removed for clarity. Representation: ball-and-stick (Cu, alkynyl, azide, and triazolyl), tube (DPEOPN), and wire (NTf_2^-). Breaking and forming bonds in $\mathbf{TS_2}$ are shown with a dotted red line (2.10 (N−C_μ) and 2.19 (N−C) Å). Bond distances in $\mathbf{6^+}$, in Å: Cu···Cu (2.38) and Cu−C_μ (2.02_P/2.03_{N2}).

The third and the last step of the CuAAC reaction consists of the proton transfer between the alkyne and $\mathbf{5^+}$, leading to the regeneration of $\mathbf{2^+}$ and the formation of the 1,4-triazole. For this step, a concerted proton transfer was assumed, similar to the one for the C−H activation of alkynes.[76] In this case, the triazolyl and the incoming alkyne can be arranged in four different isomers ($\mathbf{TS_3}$, $\mathbf{TS_4}$, $\mathbf{TS_5}$, and $\mathbf{TS_6}$ in Figure 10), depending on the approach of the alkyne (phosphine versus pyridine sides) and on the orientation of the triazolyl. With the added complexity of the partial dissociation of DPEOPN and

https://doi.org/10.1021/acscatal.2c00723
ACS Catal. 2022, 12, 4744−4753

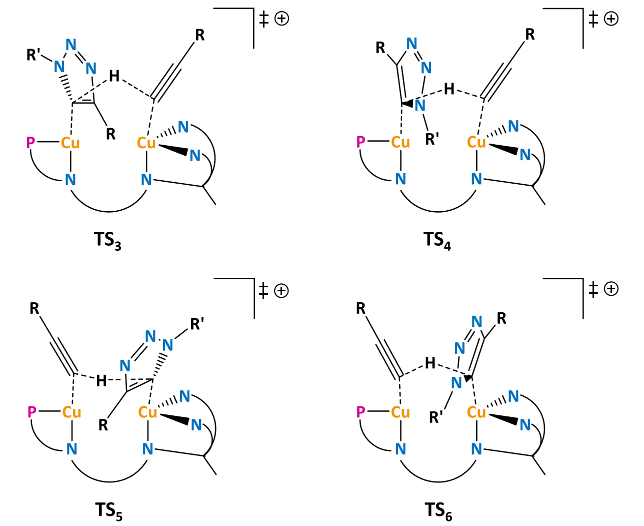

Figure 10. Different possible isomers for the transition states of the proton transfer between the alkyne and $\mathbf{5}^+$.

of the association with NTf_2^-, a total of 72 possible transition states were found for this step (Figures S15−S30).

Overall, the proton-transfer transition states yield high energy barriers, ranging from 28.7 to 42.1 kcal/mol. The lowest barrier is associated with $\mathbf{TS_{3\beta C}}$ (Figure 7B). The distinct feature of $\mathbf{TS_{3\beta C}}$ is the loose coordination of NTf_2^- in the site left by the dissociated pyridine (2.40 Å) and its interaction with both arms of DPEOPN. To accommodate the presence of the counterion, the transition state needs to distort its geometry significantly relative to the $\mathbf{5_E}$ reactant: the copper coordinated to NTf_2^- moves out of the naphthyridine plane, increasing the distance between the coppers to 3.19 Å (+0.79 Å). Another relevant change is the mode of coordination of the alkynyl, which appears bound to the two coppers in an asymmetric way, with distances of 2.17 and 2.00 Å from the coppers on the phosphine and pyridines sides, respectively. The coordination of the triazolyl is less affected as its distance increases by only 0.2 to 2.21 Å. The transferred proton is equidistant to the alkynyl and the triazolyl C atoms at 1.42 Å. The possibility of transferring the proton keeping the triazolyl ligand in the bridging position was also explored but without success because of the steric hindrance introduced by the alkyne in this hypothetical pathway.

Owing to its lowest energy barrier and structural features,$\mathbf{TS_{3\beta C}}$ highlights the importance of considering ion-pairing with NTf_2^- and the partial dissociation of DPEOPN to represent correctly the reactivity of this type of naphthyridine complexes. To be certain of the nature of these transition states, an IRC-driven relaxation was performed on their selection. Two additional intermediates were found for $\mathbf{TS_{3\beta C}}$ (Figure 11): $\mathbf{7}^+$ and $\mathbf{8}^+$, on the reactant- and product-sides of the barrier, respectively. $\mathbf{7}^+$is at 9.7 kcal/mol above $\mathbf{5}^+$ and contains the alkyne substrate coordinated to the Cu_2 core via its π-system (2.00 Å to $C_{2'}$ and 2.07 Å to $C_{3'}$). To allow for the alkyne to coordinate, the triazolyl dissociates from Cu_2 and remains coordinated to only Cu_1 (1.96 Å). $\mathbf{8}^+$ is at −10.0 kcal/mol below $\mathbf{5}^+$ and contains the 1,4 triazole product formed and dissociated from the complex. In contrast with $\mathbf{2}^+$, the alkynyl bridges the coppers asymmetrically: in σ mode to Cu_1 (1.89 Å) and in π mode to Cu_2 (2.06 Å on average). The other distinct feature of these intermediates is that the counterion remains close to Cu_2, at 2.22 and 2.51 Å for $\mathbf{7}^+$ and $\mathbf{8}^+$, respectively.

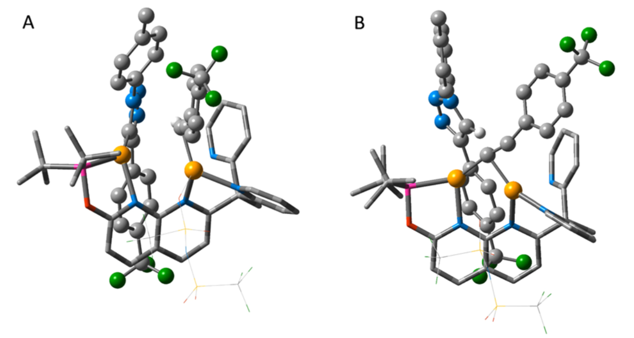

Figure 11. DFT-optimized geometries of the intermediates $\mathbf{7}^+$ (A) and $\mathbf{8}^+$ (B). All H atoms were removed for clarity, except the one involved in the C−H activation. Representation: ball-and-stick (Cu, alkynyl, azide and triazolyl), tube (DPEOPN), and wire (NTf_2^-). Selected distances, in Å, for $\mathbf{7}^+$ and $\mathbf{8}^+$, respectively: Cu···Cu (3.44, 2.85), Cu−C_{Pyr} (1.96, 3.31), and Cu−C_{alkyne} (2.00_{CH}/2.07, 2.02_{CH}/2.13).

These calculations highlight the relevance of performing the IRC exploration of the potential energy surface to reveal the existence of hidden reaction intermediates.[85]

The last topic investigated for the CuAAC reaction was the poisoning of the catalytic system. The major potential source of poisoning is the coordination of the azide to $\mathbf{2}^+$, which can occur in ways hampering the cycloaddition to the alkynyl. Thus, several off-cycle adducts shown in Figure S31 were computed. The energy reference for this section is azide + $\mathbf{2}^+$, and the energies of the intermediates are gathered in Table S4. Overall, four adducts ($\mathbf{9}_\beta^+$, $\mathbf{10}^+$, $\mathbf{10}_\beta^+$, and $\mathbf{11}_\alpha^+$, see Figure 12) were obtained, and their energies are higher than those of $\mathbf{3}^+$. In these intermediates, the azide is coordinated to the copper on the phosphine side via its terminal nitrogen. The difference between these intermediates arises from the orientation of the substituent of the azide (toward the top, near the pyridine, or close to naphthyridine) and of the coordination of DPEOPN (full or partial). The association with the counter-ion does not lead to intermediates with an energy lower than that of $\mathbf{3_E}$ and, therefore, there is no poisoning found for the CuAAC reaction. The energy profile of the full mechanism summarized in Figure 13 suggests that the RDS is the C−H activation of the alkyne. In contrast, other studies have indicated that this step is faster than the cycloaddition,[74] although for systems based on symmetric naphthyridine ligands, which, in contrast to the ligand of this study, do not differentiate the two metal centers. Our results also suggest that intermediate $\mathbf{5_E}$ could be detected experimentally, depending on the concentration of the alkyne relative to the catalyst.

CONCLUSIONS

In this work, we reported a mechanism for the CuAAC reaction starting with the coordination of the azide on Cu_1 of $\mathbf{2_B}$, forming $\mathbf{3_E}$ (Figure 13). This first step is thermoneutral (−0.8 kcal/mol) and there is no barrier other than the energy cost originating from the entropy penalty. In the next step, the alkynyl and azide ligands undergo a cycloaddition to create two C−N bonds in $\mathbf{TS1_E}$. This first transition state is moderate in energy, with a barrier of 20.0 kcal/mol, and leads to the exergonic formation (−53.9 kcal/mol) of intermediate $\mathbf{5_E}$. In contrast with previous studies, the cycloaddition follows a concerted pathway with a selectivity for the 1,4 product, consistent with experiments. The third and last steps of the

https://doi.org/10.1021/acscatal.2c00723
ACS Catal. 2022, 12, 4744−4753

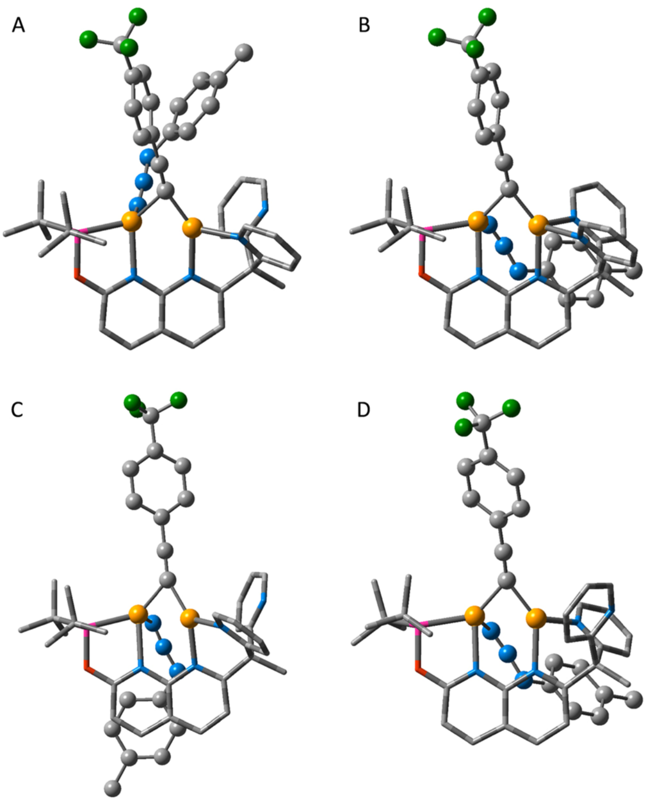

Figure 12. DFT-optimized geometries of the intermediates 9_β^+ (A), 10^+ (B), 10_β^+ (C), and 11_α^+ (D). All H atoms were removed for clarity. Representation: ball-and-stick (Cu, alkynyl, azide and triazolyl) and tube (DPEOPN). Cu−N$_{azide}$ distances, in Å, for the three intermediates: 2.12, 2.35, 2.22, and 2.43, respectively.

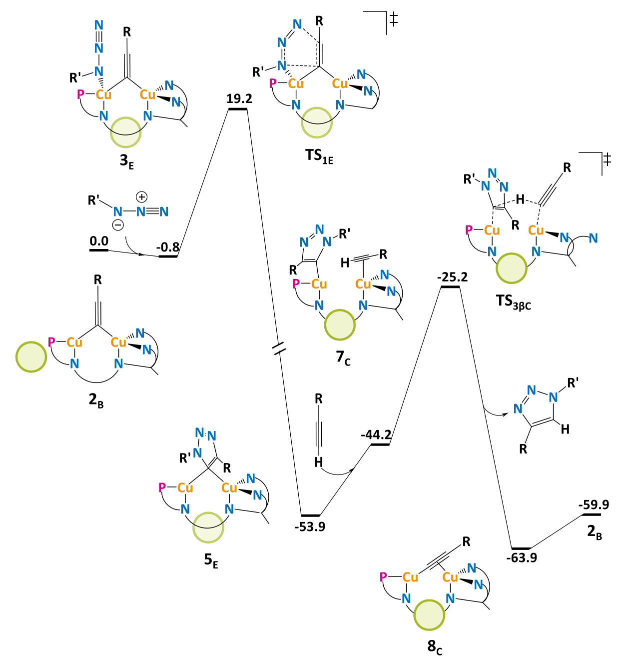

Figure 13. Catalytic cycle for the CuAAC reaction with 2^+ as the catalyst. The green spheres illustrate the position of NTf_2^- in each calculated structure.

CuAAC reaction consist of proton transfer from the alkyne to the triazolyl in 5_E, regenerating 2_B and producing the 1,4 triazole product. This step involves the highest energy barrier (28.7 kcal/mol), which is associated to the transition state $TS_{3\beta C}$. In this mechanism, the counterion plays a key role because it is bound to the copper core in the lowest-energy transition state and the two intermediates directly connected to it. There is also a clear preference for the position of NTf_2^- around the complexes: the cavity formed by the arms of DPEOPN (positions **C** and **E**), with the exception of 2_B. The partial dissociation of DPEOPN has also an important effect as it allows to lower the energy of $TS_{3\beta C}$ by 6.0 kcal/mol compared to TS_{3C}, its fully coordinated equivalent. Catalyst poisoning by coordination of the azide to 2^+ was excluded.

■ ASSOCIATED CONTENT

Supporting Information

The Supporting Information is available free of charge at https://pubs.acs.org/doi/10.1021/acscatal.2c00723.

Systematic lists of energies and charges for the stationary points associated with the reaction intermediates, coordination of the azide, cycloaddition, C−H activation, and poisoning of the catalyst (PDF)

Optimized geometries of all energy minima (reactants, intermediates, and products) and saddle points (transition states) (XYZ)

■ AUTHOR INFORMATION

Corresponding Author

David Balcells − *Hylleraas Centre for Quantum Molecular Sciences, Department of Chemistry, University of Oslo, Oslo 0315, Norway;* orcid.org/0000-0002-3389-0543; Email: david.balcells@kjemi.uio.no

Author

Julie Héron − *Hylleraas Centre for Quantum Molecular Sciences, Department of Chemistry, University of Oslo, Oslo 0315, Norway*

Complete contact information is available at: https://pubs.acs.org/10.1021/acscatal.2c00723

Notes

The authors declare no competing financial interest.

■ ACKNOWLEDGMENTS

This work was funded by the Norwegian Research Council through the Hylleraas Centre for Quantum Molecular Sciences (Project No. 262695) and the Norwegian Metacenter for Computational Science (NOTUR; Grant No. nn4654k). We thank Prof. Mats Tilset, Dr. Ainara Nova, and Prof. T. Don Tilley for helpful conversations.

■ REFERENCES

(1) Tornøe, C. W.; Christensen, C.; Meldal, M. Peptidotriazoles on Solid Phase: [1,2,3]-Triazoles by Regiospecific Copper(I)-Catalyzed 1,3-Dipolar Cycloadditions of Terminal Alkynes to Azides. *J. Org. Chem.* **2002**, *67*, 3057−3064.

(2) Rostovtsev, V. V.; Green, L. G.; Fokin, V. V.; Sharpless, K. B. A Stepwise Huisgen Cycloaddition Process: Copper(I)-Catalyzed Regioselective "Ligation" of Azides and Terminal Alkynes. *Am. Ethnol.* **2002**, *114*, 2708−2711.

(3) Liang, L.; Astruc, D. The Copper(I)-Catalyzed Alkyne-Azide Cycloaddition (CuAAC) "Click" Reaction and Its Applications. An Overview. *Coord. Chem. Rev.* **2011**, *255*, 2933−2945.

(4) Neumann, S.; Biewend, M.; Rana, S.; Binder, W. H. The CuAAC: Principles, Homogeneous and Heterogeneous Catalysts, and

Novel Developments and Applications. *Macromol. Rapid Commun.* **2020**, *41*, No. 1900359.
(5) Wang, X.; Huang, B.; Liu, X.; Zhan, P. Discovery of Bioactive Molecules from CuAAC Click-Chemistry-Based Combinatorial Libraries. *Drug Discovery Today* **2016**, *21*, 118−132.
(6) Mobian, P.; Collin, J.-P.; Sauvage, J.-P. Efficient Synthesis of a Labile Copper(I)-Rotaxane Complex Using Click Chemistry. *Tetrahedron Lett.* **2006**, *47*, 4907−4909.
(7) Lee, J. W.; Kim, B.-K.; Kim, J.-H.; Shin, W. S.; Jin, S.-H. Facile Synthesis of Fréchet Type Dendritic Benzyl Azides and Dendrimer via Cycloaddition Reaction with Tripodal Core. *Bull. Korean Chem. Soc.* **2005**, *26*, 1790−1794.
(8) Megiatto, J. D.; Schuster, D. I. General Method for Synthesis of Functionalized Macrocycles and Catenanes Utilizing "Click" Chemistry. *J. Am. Chem. Soc.* **2008**, *130*, 12872−12873.
(9) Jiang, X.; Hao, X.; Jing, L.; Wu, G.; Kang, D.; Liu, X.; Zhan, P. Recent Applications of Click Chemistry in Drug Discovery. *Expert Opin. Drug Discovery* **2019**, *14*, 779−789.
(10) Ornelas, C.; Ruiz, J.; Salmon, L.; Astruc, D. Sulphonated "Click" Dendrimer-Stabilized Palladium Nanoparticles as Highly Efficient Catalysts for Olefin Hydrogenation and Suzuki Coupling Reactions Under Ambient Conditions in Aqueous Media. *Adv. Synth. Catal.* **2008**, *350*, 837−845.
(11) Lee, J. W.; Kim, J. H.; Kim, B.-K.; Shin, W. S.; Jin, S.-H. Synthesis of Fréchet Type Dendritic Benzyl Propargyl Ether and Fréchet Type Triazole Dendrimer. *Tetrahedron* **2006**, *62*, 894−900.
(12) Loethen, S.; Ooya, T.; Choi, H. S.; Yui, N.; Thompson, D. H. Synthesis, Characterization, and PH-Triggered Dethreading of α-Cyclodextrin-Poly(Ethylene Glycol) Polyrotaxanes Bearing Cleavable Endcaps. *Biomacromolecules* **2006**, *7*, 2501−2506.
(13) Döhler, D.; Michael, P.; Binder, W. H. CuAAC-Based Click Chemistry in Self-Healing Polymers. *Acc. Chem. Res.* **2017**, *50*, 2610−2620.
(14) Castro, V.; Rodríguez, H.; Albericio, F. CuAAC: An Efficient Click Chemistry Reaction on Solid Phase. *ACS Comb. Sci.* **2016**, *18*, 1−14.
(15) Tasdelen, M. A. Diels−Alder "Click" Reactions: Recent Applications in Polymer and Material Science. *Polym. Chem.* **2011**, *2*, 2133.
(16) Yang, C.; Flynn, J. P.; Niu, J. Facile Synthesis of Sequence-Regulated Synthetic Polymers Using Orthogonal SuFEx and CuAAC Click Reactions. *Angew. Chem., Int. Ed.* **2018**, *57*, 16194−16199.
(17) Meldal, M. Polymer "Clicking" by CuAAC Reactions. *Macromol. Rapid Commun.* **2008**, *29*, 1016−1051.
(18) Zhang, H.; Zhu, Y.; Chen, J.; Zhang, S. Preparation of PolyHIPE via CuAAC "Click" Chemistry and Its Application as a Highly Efficient Adsorbent of Cu(II) Ions. *J. Polym. Sci., Part A: Polym. Chem.* **2017**, *55*, 2129−2135.
(19) Huang, Z.; Zhou, Y.; Wang, Z.; Li, Y.; Zhang, W.; Zhou, N.; Zhang, Z.; Zhu, X. Recent Advances of CuAAC Click Reaction in Building Cyclic Polymer. *Chin. J. Polym. Sci.* **2017**, *35*, 317−341.
(20) Chassaing, S.; Bénéteau, V.; Pale, P. When CuAAC "Click Chemistry" Goes Heterogeneous. *Catal. Sci. Technol.* **2016**, *6*, 923−957.
(21) Lutz, J.; Zarafshani, Z. Efficient Construction of Therapeutics, Bioconjugates, Biomaterials and Bioactive Surfaces Using Azide−Alkyne "Click" Chemistry. *Adv. Drug Delivery Rev.* **2008**, *60*, 958−970.
(22) Chen, J.; Wang, J.; Li, K.; Wang, Y.; Gruebele, M.; Ferguson, A. L.; Zimmerman, S. C. Polymeric "Clickase" Accelerates the Copper Click Reaction of Small Molecules, Proteins, and Cells. *J. Am. Chem. Soc.* **2019**, *141*, 9693−9700.
(23) Oyman Eyrilmez, G.; Doran, S.; Murtezi, E.; Demir, B.; Odaci Demirkol, D.; Coskunol, H.; Timur, S.; Yagci, Y. Selective Cell Adhesion and Biosensing Applications of Bio-Active Block Copolymers Prepared by CuAAC/Thiol-Ene Double Click Reactions. *Macromol. Biosci.* **2015**, *15*, 1233−1241.
(24) Debiais, M.; Vasseur, J.-J.; Müller, S.; Smietana, M. Selective Chemical Modification of DNA with Boronic Acids by On-Column CuAAc Reactions. *Synthesis* **2020**, *52*, 2962−2969.
(25) Sun, N.; Yu, Z.; Yi, H.; Zhu, X.; Jin, L.; Hu, B.; Shen, Z.; Hu, X. Synthesis of a Heterogeneous $Cu(OAc)_2$-Anchored SBA-15 Catalyst and Its Application in the CuAAC Reaction. *New J. Chem.* **2018**, *42*, 1612−1616.
(26) Xiao, J.; Tolbert, T. J. Synthesis of N-Terminally Linked Protein Dimers and Trimers by a Combined Native Chemical Ligation-CuAAC Click Chemistry Strategy. *Org. Lett.* **2009**, *11*, 4144−4147.
(27) Slavíčková, M.; Janoušková, M.; Šimonová, A.; Cahová, H.; Kambová, M.; Šanderová, H.; Krásný, L.; Hocek, M. Turning Off Transcription with Bacterial RNA Polymerase through CuAAC Click Reactions of DNA Containing 5-Ethynyluracil. *Chem. − Eur. J.* **2018**, *24*, 8311−8314.
(28) Kolb, H. C.; Finn, M. G.; Sharpless, K. B. Click Chemistry: Diverse Chemical Function from a Few Good Reactions. *Angew. Chem., Int. Ed.* **2001**, *40*, 2004−2021.
(29) (a) Haldón, E.; Nicasio, M. C.; Pérez, P. J. Copper-Catalysed Azide−Alkyne Cycloadditions (CuAAC): An Update. *Org. Biomol. Chem.* **2015**, *13*, 9528−9550. (b) Haldon, E.; Besora, M.; Cano, I.; Cambeiro, X. C.; Pericas, M. A.; Maseras, F.; Nicasio, M. C.; Perez, P. J. Reaction of Alkynes and Azides: Not Triazoles Through Copper-Acetylides but Oxazoles Through Copper-Nitrene Intermediates. *Chem. − Eur. J.* **2014**, *20*, 3463−3474.
(30) Hein, J. E.; Fokin, V. V. Copper-Catalyzed Azide−Alkyne Cycloaddition (CuAAC) and beyond: New Reactivity of Copper(I) Acetylides. *Chem. Soc. Rev.* **2010**, *39*, 1302−1315.
(31) Bock, V. D.; Hiemstra, H.; van Maarseveen, J. H. CuI-Catalyzed Alkyne−Azide "Click" Cycloadditions from a Mechanistic and Synthetic Perspective. *Eur. J. Org. Chem.* **2006**, *2006*, 51−68.
(32) Zhu, L.; Brassard, C. J.; Zhang, X.; Guha, P. M.; Clark, R. J. On the Mechanism of Copper(I)-Catalyzed Azide-Alkyne Cycloaddition. *Chem. Rec.* **2016**, *16*, 1501−1517.
(33) Meldal, M.; Diness, F. Recent Fascinating Aspects of the CuAAC Click Reaction. *Trends Chem.* **2020**, *2*, 569−584.
(34) Díez-González, S. Well-Defined Copper(I) Complexes for Click Azide−Alkyne Cycloaddition Reactions: One Click Beyond. *Catal. Sci. Technol.* **2011**, *1*, 166−178.
(35) Patil, P. C.; Luzzio, F. A. Alternate Pathway for the Click Reaction of 2-(2-Azidophenyl)-4,5-Diaryloxazoles. *Tetrahedron Lett.* **2018**, *59*, 3458−3460.
(36) Peng, H.; Dornevil, K. H.; Draganov, A. B.; Chen, W.; Dai, C.; Nelson, W. H.; Liu, A.; Wang, B. An Unexpected Copper Catalyzed 'Reduction' of an Arylazide to Amine through the Formation of a Nitrene Intermediate. *Tetrahedron* **2013**, *69*, 5079−5085.
(37) Yoo, E. J.; Ahlquist, M.; Kim, S. H.; Bae, I.; Fokin, V. V.; Sharpless, K. B.; Chang, S. Copper-Catalyzed Synthesis OfN-Sulfonyl-1,2,3-Triazoles: Controlling Selectivity. *Angew. Chem., Int. Ed.* **2007**, *46*, 1730−1733.
(38) Yoo, E. J.; Ahlquist, M.; Bae, I.; Sharpless, K. B.; Fokin, V. V.; Chang, S. Mechanistic Studies on the Cu-Catalyzed Three-Component Reactions of Sulfonyl Azides, 1-Alkynes and Amines, Alcohols, or Water: Dichotomy via a Common Pathway. *J. Org. Chem.* **2008**, *73*, 5520−5528.
(39) Himo, F.; Lovell, T.; Hilgraf, R.; Rostovtsev, V. V.; Noodleman, L.; Sharpless, K. B.; Fokin, V. V. Copper(I)-Catalyzed Synthesis of Azoles. DFT Study Predicts Unprecedented Reactivity and Intermediates. *J. Am. Chem. Soc.* **2005**, *127*, 210−216.
(40) Nolte, C.; Mayer, P.; Straub, B. F. Isolation of a Copper(I) Triazolide: A "Click" Intermediate. *Angew. Chem., Int. Ed.* **2007**, *46*, 2101−2103.
(41) Calvo-Losada, S.; Pino, M. S.; Quirante, J. J. On the Regioselectivity of the Mononuclear Copper-Catalyzed Cycloaddition of Azide and Alkynes (CuAAC). A Quantum Chemical Topological Study. *J. Mol. Model.* **2014**, *20*, 2187−2193.

(42) Rodionov, V. O.; Fokin, V. V.; Finn, M. G. Mechanism of the Ligand-Free CuI-Catalyzed Azide-Alkyne Cycloaddition Reaction. *Am. Ethnol.* **2005**, *117*, 2250−2255.

(43) Straub, B. F. μ-Acetylide and μ-Alkenylidene Ligands in "Click" Triazole Syntheses. *Chem. Commun.* **2007**, *37*, 3868−3870.

(44) Ahlquist, M.; Fokin, V. V. Enhanced Reactivity of Dinuclear Copper(I) Acetylides in Dipolar Cycloadditions. *Organometallics* **2007**, *26*, 4389−4391.

(45) Kamata, K.; Nakagawa, Y.; Yamaguchi, K.; Mizuno, N. 1,3-Dipolar Cycloaddition of Organic Azides to Alkynes by a Dicopper-Substituted Silicotungstate. *J. Am. Chem. Soc.* **2008**, *130*, 15304−15310.

(46) Cantillo, D.; Ávalos, M.; Babiano, R.; Cintas, P.; Jiménez, J. L.; Palacios, J. C. Assessing the Whole Range of CuAAC Mechanisms by DFT Calculations—on the Intermediacy of Copper Acetylides. *Org. Biomol. Chem.* **2011**, *9*, 2952−2958.

(47) Straub, B. F.; Bessel, M.; Berg, R. Dicopper Catalysts for the Azide Alkyne Cycloaddition: A Mechanistic DFT Study. In *Modeling of Molecular Properties*; Comba, P., Ed.; Wiley-VCH Verlag GmbH & Co. KGaA: Weinheim, Germany, 2011; pp 207−214.

(48) Calvo-Losada, S.; Pino-González, M. S.; Quirante, J. J. Rationalizing the Catalytic Activity of Copper in the Cycloaddition of Azide and Alkynes (CuAAC) with the Topology of $\nabla 2\rho(r)$ and $\nabla\nabla 2\rho(r)$. *J. Phys. Chem. B* **2015**, *119*, 1243−1258.

(49) (a) Özkılıç, Y.; Tüzün, N. Ş. A DFT Study on the Binuclear CuAAC Reaction: Mechanism in Light of New Experiments. *Organometallics* **2016**, *35*, 2589−2599. (b) Peng, L.; Gu, F. G. Mechanistic understanding of the Cu(I)-catalyzed domino reaction constructing 1-aryl-1,2,3-triazole from electron-rich aryl bromide, alkyne, and sodium azide: a DFT study. *Catal. Sci. Technol.* **2021**, *11*, 3208−3216.

(50) Kalvet, I.; Tammiku-Taul, J.; Mäeorg, U.; Tämm, K.; Burk, P.; Sikk, L. NMR and DFT Study of the Copper(I)-Catalyzed Cycloaddition Reaction: H/D Scrambling of Alkynes and Variable Reaction Order of the Catalyst. *ChemCatChem* **2016**, *8*, 1804−1808.

(51) Jin, L.; Tolentino, D. R.; Melaimi, M.; Bertrand, G. Isolation of Bis(Copper) Key Intermediates in Cu-Catalyzed Azide-Alkyne "Click Reaction.". *Sci. Adv.* **2015**, *1*, No. e1500304.

(52) Buckley, B. R.; Dann, S. E.; Heaney, H. Experimental Evidence for the Involvement of Dinuclear Alkynyl Copper(I) Complexes in Alkyne-Azide Chemistry. *Chem. − Eur. J.* **2010**, *16*, 6278−6284.

(53) Kuang, G.-C.; Guha, P. M.; Brotherton, W. S.; Simmons, J. T.; Stankee, L. A.; Nguyen, B. T.; Clark, R. J.; Zhu, L. Experimental Investigation on the Mechanism of Chelation-Assisted, Copper(II) Acetate-Accelerated Azide−Alkyne Cycloaddition. *J. Am. Chem. Soc.* **2011**, *133*, 13984−14001.

(54) Worrell, B. T.; Malik, J. A.; Fokin, V. V. Direct Evidence of a Dinuclear Copper Intermediate in Cu(I)-Catalyzed Azide-Alkyne Cycloadditions. *Science* **2013**, *340*, 457−460.

(55) Makarem, A.; Berg, R.; Rominger, F.; Straub, B. F. A Fluxional Copper Acetylide Cluster in CuAAC Catalysis. *Angew. Chem., Int. Ed.* **2015**, *54*, 7431−7435.

(56) Iacobucci, C.; Reale, S.; Gal, J.-F.; De Angelis, F. Dinuclear Copper Intermediates in Copper(I)-Catalyzed Azide-Alkyne Cycloaddition Directly Observed by Electrospray Ionization Mass Spectrometry. *Angew. Chem., Int. Ed.* **2015**, *54*, 3065−3068.

(57) Iacobucci, C.; Lebon, A.; De Angelis, F.; Memboeuf, A. CuAAC Click Reactions in the Gas Phase: Unveiling the Reactivity of Bis-Copper Intermediates. *Chem. − Eur. J.* **2016**, *22*, 18690−18694.

(58) Brotherton, W. S.; Michaels, H. A.; Simmons, J. T.; Clark, R. J.; Dalal, N. S.; Zhu, L. Apparent Copper(II)-Accelerated Azide−Alkyne Cycloaddition. *Org. Lett.* **2009**, *11*, 4954−4957.

(59) Özen, C.; Tüzün, N. Ş. The Mechanism of Copper-Catalyzed Azide−Alkyne Cycloaddition Reaction: A Quantum Mechanical Investigation. *J. Mol. Graphics Modell.* **2012**, *34*, 101−107.

(60) Özen, C.; Tüzün, N. Ş. Mechanism of CuAAC Reaction: In Acetic Acid and Aprotic Conditions. *J. Mol. Catal. Chem.* **2017**, *426*, 150−157.

(61) Chen, H.; Soubra-Ghaoui, C.; Zhu, Z.; Li, S.; Albright, T. A.; Cai, C. Isolation of an Acetylide-CuI3-Tris(Triazolylmethyl)Amine Complex Active in the CuAAC Reaction. *J. Catal.* **2018**, *361*, 407−413.

(62) Calvo-Losada, S.; Quirante, J. J. Exploring the Regioselectivity in the Cycloaddition of Azides to Alkynes Catalyzed by Dinuclear Copper Clusters (Cu2AAC Reaction) Using the Topologies of $\nabla 2\rho(r)$ and $\nabla\nabla 2\rho(r)$. *J. Mol. Model.* **2017**, *23*, 337.

(63) Shao, C.; Cheng, G.; Su, D.; Xu, J.; Wang, X.; Hu, Y. Copper(I) Acetate: A Structurally Simple but Highly Efficient Dinuclear Catalyst for Copper-Catalyzed Azide-Alkyne Cycloaddition. *Adv. Synth. Catal.* **2010**, *352*, 1587−1592.

(64) Jin, L.; Romero, E. A.; Melaimi, M.; Bertrand, G. The Janus Face of the X Ligand in the Copper-Catalyzed Azide−Alkyne Cycloaddition. *J. Am. Chem. Soc.* **2015**, *137*, 15696−15698.

(65) Díez-González, S.; Correa, A.; Cavallo, L.; Nolan, S. P. (NHC)Copper(I)-Catalyzed [3+2] Cycloaddition of Azides and Mono- or Disubstituted Alkynes. *Chem. − Eur. J.* **2006**, *12*, 7558−7564.

(66) Díez-González, S.; Nolan, S. P. [(NHC)2Cu]X Complexes as Efficient Catalysts for Azide-Alkyne Click Chemistry at Low Catalyst Loadings. *Angew. Chem., Int. Ed. Engl.* **2008**, *47*, 8881−8884.

(67) Berg, R.; Straub, J.; Schreiner, E.; Mader, S.; Rominger, F.; Straub, B. F. Highly Active Dinuclear Copper Catalysts for Homogeneous Azide-Alkyne Cycloadditions. *Adv. Synth. Catal.* **2012**, *354*, 3445−3450.

(68) Lewis, W. G.; Magallon, F. G.; Fokin, V. V.; Finn, M. G. Discovery and Characterization of Catalysts for Azide−Alkyne Cycloaddition by Fluorescence Quenching. *J. Am. Chem. Soc.* **2004**, *126*, 9152−9153.

(69) Chan, T. R.; Hilgraf, R.; Sharpless, K. B.; Fokin, V. V. Polytriazoles as Copper(I)-Stabilizing Ligands in Catalysis. *Org. Lett.* **2004**, *6*, 2853−2855.

(70) Rodionov, V. O.; Presolski, S. I.; Gardinier, S.; Lim, Y.-H.; Finn, M. G. Benzimidazole and Related Ligands for Cu-Catalyzed Azide−Alkyne Cycloaddition. *J. Am. Chem. Soc.* **2007**, *129*, 12696−12704.

(71) Rodionov, V. O.; Presolski, S. I.; Díaz, D.; Fokin, V. V.; Finn, M. G. Ligand-Accelerated Cu-Catalyzed Azide−Alkyne Cycloaddition: A Mechanistic Report. *J. Am. Chem. Soc.* **2007**, *129*, 12705−12712.

(72) Presolski, S. I.; Hong, V.; Cho, S.-H.; Finn, M. G. Tailored Ligand Acceleration of the Cu-Catalyzed Azide−Alkyne Cycloaddition Reaction: Practical and Mechanistic Implications. *J. Am. Chem. Soc.* **2010**, *132*, 14570−14576.

(73) Gonda, Z.; Novák, Z. Highly Active Copper-Catalysts for Azide-Alkynecycloaddition. *Dalton Trans.* **2010**, *39*, 726−729.

(74) (a) Ziegler, M. S.; Lakshmi, K. V.; Tilley, T. D. Dicopper Cu(I)Cu(I) and Cu(I)Cu(II) Complexes in Copper-Catalyzed Azide−Alkyne Cycloaddition. *J. Am. Chem. Soc.* **2017**, *139*, 5378−5386. (b) Desnoyer, A. N.; Nicolay, A.; Rios, P.; Ziegler, M. S.; Tilley, T. D. Bimetallics in a Nutshell: Complexes Supported by Chelating Naphthyridine-Based Ligands. *Acc. Chem. Res.* **2020**, *53*, 1944−1956.

(75) Saha, S.; Kaur, M.; Bera, J. K. Fluorinated Anions Promoted "on Water" Activity of Di- and Tetranuclear Copper(I) Catalysts for Functional Triazole Synthesis. *Organometallics* **2015**, *34*, 3047−3054.

(76) Nicolay, A.; Héron, J.; Shin, C.; Ziegler, M. S.; Balcells, D.; Tilley, T. D. Unsymmetrical Naphthyridine-Based Dicopper(I) Complexes - Synthesis, Stability, and Carbon−Hydrogen Bond Activations. *Organometallics* **2021**, *40*, 1866−1873.

(77) Adamo, C.; Barone, V. Toward Reliable Density Functional Methods without Adjustable Parameters: The PBE0 Model. *J. Chem. Phys.* **1999**, *110*, 6158−6170.

(78) Frisch, M. J.; Trucks, G. W.; Schlegel, H. B.; Scuseria, G. E.; Robb, M. A.; Cheeseman, J. R.; Scalmani, G.; Barone, V.; Petersson, G. A.; Nakatsuji, H.; Li, X.; Caricato, M.; Marenich, A. V.; Bloino, J.; Janesko, B. G.; Gomperts, R.; Mennucci, B.; Hratchian, H. P.; Ortiz, J. V.; Izmaylov, A. F.; Sonnenberg, J. L.; Williams-Young, D.; Ding, F.; Lipparini, F.; Egidi, F.; Goings, J.; Peng, B.; Petrone, A.; Henderson, T.; Ranasinghe, D.; Zakrzewski, V. G.; Gao, J.; Rega, N.; Zheng, G.;

https://doi.org/10.1021/acscatal.2c00723
ACS Catal. 2022, 12, 4744−4753

Liang, W.; Hada, M.; Ehara, M.; Toyota, K.; Fukuda, R.; Hasegawa, J.; Ishida, M.; Nakajima, T.; Honda, Y.; Kitao, O.; Nakai, H.; Vreven, T.; Throssell, K.; Montgomery, J. A., Jr.; Peralta, J. E.; Ogliaro, F.; Bearpark, M. J.; Heyd, J. J.; Brothers, E. N.; Kudin, K. N.; Staroverov, V. N.; Keith, T. A.; Kobayashi, R.; Normand, J.; Raghavachari, K.; Rendell, A. P.; Burant, J. C.; Iyengar, S. S.; Tomasi, J.; Cossi, M.; Millam, J. M.; Klene, M.; Adamo, C.; Cammi, R.; Ochterski, J. W.; Martin, L. R.; Morokuma, K.; Farkas, O.; Foresman, J. B.; Fox, D. J. *Gaussian 16*; Gaussian, Inc.: Wallingford CT, 2016.

(79) Grimme, S.; Antony, J.; Ehrlich, S.; Krieg, H. A Consistent and Accurate Ab Initio Parametrization of Density Functional Dispersion Correction (DFT-D) for the 94 Elements H-Pu. *J. Chem. Phys.* **2010**, *132*, 154104.

(80) Weigend, F. Accurate Coulomb-Fitting Basis Sets for H to Rn. *Phys. Chem. Chem. Phys.* **2006**, *8*, 1057.

(81) Weigend, F.; Ahlrichs, R. Balanced Basis Sets of Split Valence, Triple Zeta Valence and Quadruple Zeta Valence Quality for H to Rn: Design and Assessment of Accuracy. *Phys. Chem. Chem. Phys.* **2005**, *7*, 3297−3305.

(82) Cossi, M.; Rega, N.; Scalmani, G.; Barone, V. Energies, Structures, and Electronic Properties of Molecules in Solution with the C-PCM Solvation Model. *J. Comput. Chem.* **2003**, *24*, 669−681.

(83) Barone, V.; Cossi, M. Quantum Calculation of Molecular Energies and Energy Gradients in Solution by a Conductor Solvent Model. *J. Phys. Chem. A* **1998**, *102*, 1995−2001.

(84) de Boer, S. Y.; Gloaguen, Y.; Lutz, M.; van der Vlugt, J. I. CuI Click Catalysis with Cooperative Noninnocent Pyridylphosphine Ligands. *Inorg. Chim. Acta* **2012**, *380*, 336−342.

(85) (a) Kraka, E.; Cremer, D. Computational Analysis of the Mechanism of Chemical Reactions in Terms of Reaction Phases: Hidden Intermediates and Hidden Transition States. *Acc. Chem. Res.* **2010**, *43*, 591−601. (b) Lal, S.; Rzepa, H. S.; Díez-González, S. Catalytic and Computational Studies of N-Heterocyclic Carbene or Phosphine-Containing Copper(I) Complexes for the Synthesis of 5-Iodo-1,2,3-Triazoles. *ACS Catal.* **2014**, *4*, 2274−2287.

https://doi.org/10.1021/acscatal.2c00723
ACS Catal. 2022, 12, 4744−4753